

Offshore wind turbine installation vessel dynamic positioning capability analysis with considering installation structures

Daeseong Lim¹, S.W. Kim^{*2}, Jeong-Hyun Yoon¹ and Seo-ho Lee¹

¹*Intelligent Mechatronics Engineering, Sejong University, 209, Neungdong-ro, Gwangjin-gu, Seoul, Republic of Korea*

²*Intelligent Mechatronics Engineering, Sejong University, 209, Neungdong-ro, Gwangjin-gu, Seoul, Republic of Korea*

(Received October 7, 2022, Revised November 21, 2022, Accepted December 17, 2022)

Abstract. Dynamic Positioning (DP) is a system that uses computer-controlled thrusters, propellers, and other propulsion devices to automatically maintain a vessel's position and heading. In this study, a wind turbine installation vessel with DP capabilities was proposed for use in mild environmental conditions in the Yellow Sea. The thruster arrangements of the vessel were analyzed in relation to wind and current loads, and it was found that a four-corner arrangement of thrusters provided the best position-keeping performance. The vessel's DP control performance was also analyzed in relation to the increased environmental load caused by the presence of a wind turbine, using a capability plot. The vessel's performance was evaluated in three different states: floating with no load, during the loading of a wind turbine and suction buckets, and after the wind turbine has been installed. The use of 750 kW and 1,000 kW thrusters was also considered, and the environmental loads in the Saemangeum coastal area and the environmental load when a 5-Megawatt wind turbine is on board were assessed. The study concluded that at least four thrusters should be used for DP to safely manage the installation process of wind turbines.

Keywords: capability plot; computational fluid dynamics; dynamic positioning; wind turbine installation vessel

1. Introduction

The demand for renewable energy has increased globally due to concerns about climate change. According to the 2021 Net Zero by 2050 report released by International Energy Agency, a global energy forecaster, 80% of global energy supplies are now produced using fossil fuels (Tsiropoulos *et al.* 2020). In an effort to address this issue, the Republic of Korea is planning to build a 20 GW offshore wind farm in the Southwest Sea by 2034. However, building wind farms in deep water and open sea areas can be challenging due to the influence of larger environmental factors on ships. To install the wind turbines, the suction bucket technology will be used, which involves using a hole in the support pile to pump out water and insert the pile into the seabed, reducing noise and vibration problems and reducing the time required for installation (DFI 2017).

Due to the deep water and open sea locations of the planned wind farm, ships will be subjected

*Corresponding author, Assistant Professor, E-mail: sewonkim@sejong.ac.kr

to larger environmental factors. Therefore, research on the motor characteristics and automatic position control technology of marine structures, including the Dynamic Positioning System (DPS), has been conducted worldwide (Mahfouz, A.B. and H.W. El-Tahan 2006, Tannuri *et al.* 2010) and developed (Hyakudome *et al.* 1999, Mun-Keun 2001, Choi *et al.* 2012).

For dynamic positioning, Dr. S.W. Kim's research that focuses on energy usage thrust algorithm is proposed. (Kim 2016) and conducted a study on Moored FPSO vessel's Turret location impact (Kim *et al.* 2016).

Previous studies have focused on the transportation and installation stability of breakwater caissons using a floating block (Seok *et al.* 2010) and dynamic movement under marine environmental conditions (Webb 1998, Jo 2009). In 2006, there was a study comparing the results of simulation and actual performance to improve the technology of Floating Over Deck (FOD) installation (Tahar *et al.* 2006), and Dr. Azian proves that floating installation DP2 vessels technically feasible (Abu Bakar *et al.* 2019), dynamic movement under marine environmental conditions (Jo 2009) and computerized hydrodynamic analysis of jack-up loads. However, little consideration has been given to the shape of the marine installation structure and its impact on the load of the installation vessel.

In particular, in the case of wind turbine installation vessels, research was conducted in 2018 to minimize costs in the process of constructing wind farms (Paterson *et al.* 2018). In that study, the cost of the installation vessel during the installation process was calculated as the average value. In 2020, an experiment was conducted to analyze the load by changing the jacking method for a vessel using the jacking installation method (Bai *et al.* 2010, Valčić 2020). And there is a paper that studies the forces acting on the boat and caissons that were mounted on a floating transportation barge and towed by a tug boat considering both the frequency-domain approach and time-domain (Kang and Kim 2014).

In this study, a barge-type wind turbine installation vessel is modeled and analyzed, considering the shape of the installation structure. The additional forces generated by the installation structure using the suction bucket system are also analyzed.

2. Materials and method

2.1 Experiment cases

In this study, we examined the process of installing a 5 MW wind turbine as part of the construction of an offshore wind farm in Saemangeum, South Korea. The installation process consists of the following steps:

1. The fully assembled wind turbine and foundation are transported to the installation site using a specialized vessel.
2. The heading angle of the vessel is controlled using a DPS to ensure the required orientation of the wind turbine.
3. the foundation and suction bucket are detached and lowered while the wind turbine remains on the vessel.
4. The wind turbine is gradually lowered and connected to the foundation.

The vessel used in this study, which is of the barge type, has the specifications listed in Table 1. To analyze the ability of the wind turbine installation vessel to maintain its position while carrying

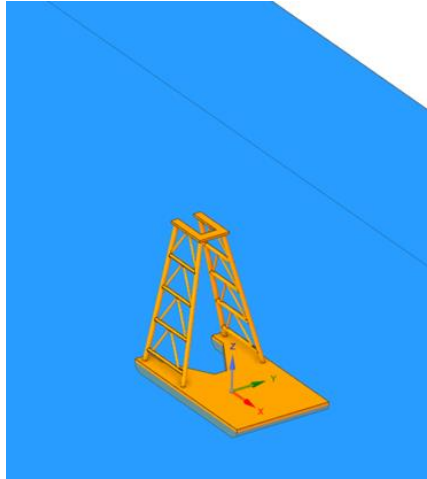


Fig. 1 Analysis state 1. Hull

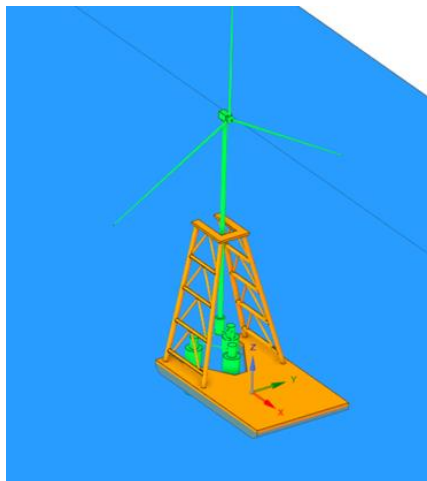


Fig. 2 Analysis state 2. Wind turbine

the installation structure, we divided the vessel's operation into three phases: no load, 5 MW wind turbine with suction buckets attached, and operation with suction buckets removed (as shown in Figs. 1-3). In addition, the installation vessel used in the Saemangeum area employs ballast tanks to adjust its draught for optimal thrust and stability. Therefore, all three phases were analyzed at the same draught in this analysis.

2.2 Environments

This study simulated the potential installation of wind power turbines in the Saemangeum coastal region near the city of Gunsan in South Korea (as depicted in Fig. 4).

To create the simulation environment, the authors utilized weather data from the Korea Meteorological Administration for a three-year period, which showed an average winter wind speed

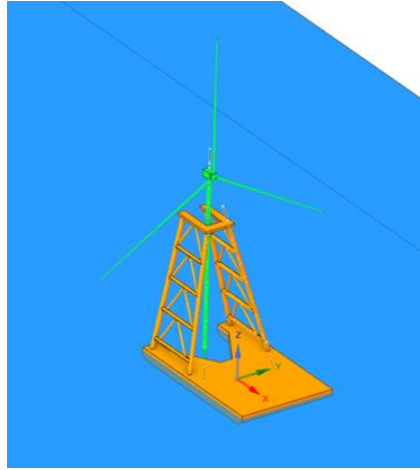


Fig. 3 Analysis state 3. Install Operation (Suction bucket dropped)

Table 1 Principal Dimension of the vessel

Item	Principal Dimensions	
Length overall	m	72
Breadth	m	45
Draught(not using ballast)	m	1.4
Draught(using ballast)	m	3.7
Displacement	m ³	11,748

Table 2 Principal Dimension of the Wind Turbine

Item	Principal Dimensions	
Number of blades	-	3
Rotor diameter	m	126
Rated power	MW	5.0
Hub height	m	90
Hub diameter	m	3
Single blade weight	ton	21.4
Nacelle weight	ton	277.0

Table 3 Principal Dimension of the Suction bucket

Item	Principal Dimensions	
Foundation type	Tripod	
Foundation diameter	m	7.0
Foundation height	m	20.0
Suction cylinder diameter	m	3.5
Suction cylinder height	m	5.0
Mounted point	m	59.5 (From bow)

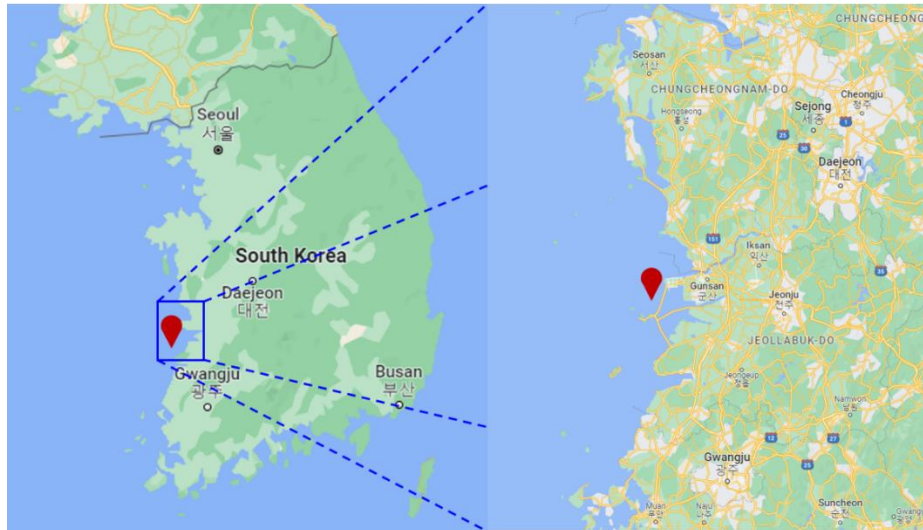


Fig. 4 Operation test-bed area (Gunsan Saemangeum)

Table 4 Environmental Information

Item	Principal Dimensions
Wind speed	7.4 m/s
Wind angle	0°~360°
Current speed	1.8 m/s
Current angle	70°, 240°

To create the simulation environment, the authors utilized weather data from the Korea Meteorological Administration for a three-year period, which showed an average winter wind speed in the Saemangeum area of approximately 7.0 m/s and an average annual wind speed of around 4.9 m/s. Additionally, the authors used monthly data on the highest flow speeds at the Gunsan Port in 2020, which reached a maximum of 1.9 m/s in January and had a daily average flow speed of 1.0 m/s. The environmental conditions used in this study are summarized in Table 4.

2.3 Thrusters

The performance of thrusters, an omnidirectional propulsion system, was evaluated for their ability to maintain the position of a wind turbine vessel. These thrusters are capable of producing a maximum thrust of 160 kN at a power output of 1000 kW for a single thruster, or 120 kN at 750 kW. The authors conducted tests on vessels with three or four propellers installed. Figs. 5 and 6 show the configurations with three and four propellers, respectively, while Fig. 7 depicts the arrangement with four propellers installed in the corners.

2.4 Governing equation

The mass and momentum conservation equation for a three-dimensional, incompressible fluid

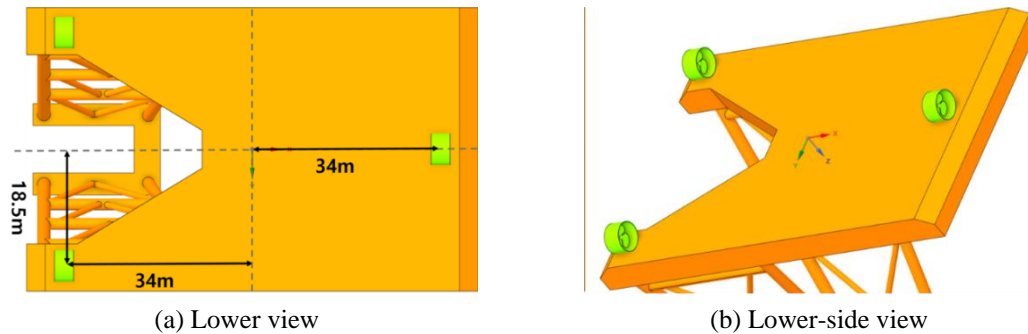


Fig. 5 Thruster Configuration 1. three thrusters in use

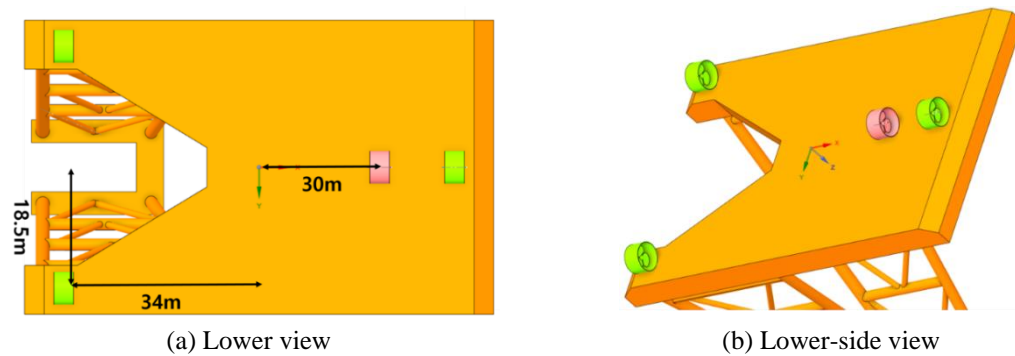


Fig. 6 Thruster Configuration 2. four thrusters in use

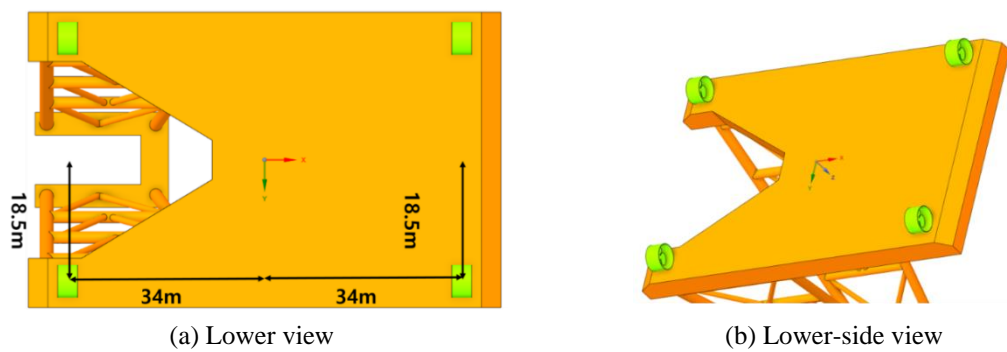


Fig. 7 Thruster Configuration 3. four thrusters at corners in use

was used to govern the analysis. A vessel-fixed coordinate system was employed using a Computational Fluid Dynamics (CFD) tool to calculate the stress around the vessel. The fluid was rotated every 15° with the midship as the center, and the wind and current were always set to act in the same direction.

The detailed analysis conditions used for the CFD analysis are provided in the Table 5 below. This governing equation results in an analysis with minimal turbulence effects, as the analysis model does not have a dynamically changing streamlined shape and the static analysis area does not experience acceleration.

Table 5 Numerical schemes and boundary conditions

Item	Content	
CFD tool	Fluent 2021-R2 CFD Solver	
Solver Type	Pressure based	
Turbulent model	Model	$\kappa - \omega$ SST
	Intensity	5%
	Viscosity Ratio	10
Wall function	standard wall function	
Boundary conditions	Inlet	Velocity
	Outlet	Pressure
Hull and structure	Non-slip	

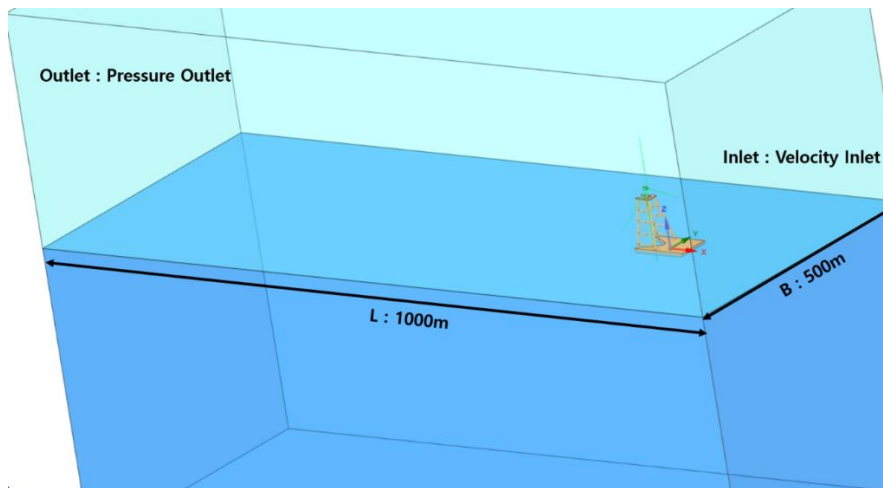


Fig. 8 Boundary condition

2.5 Grid and boundary condition

In order to ensure that the wall effect did not impact the analysis, the size of the fluid was set to be large enough in this study. To prevent the shape from being distorted on the surface of the wind turbine and vessel, the minimum mesh size was set to 0.15 m and the growth rate was set to 1.2. The boundary condition is shown in Fig. 8, and examples of the grids can be seen in Figs. 9 and 10.

3. Result

3.1 Environmental load analysis

Typically, the pressure distribution around a vessel and a structure is expressed as the sum of static pressure, hydrostatic pressure, and dynamic pressure. However, in this chapter, only static pressure and dynamic pressure are depicted, as calculated using Ansys Fluent. The average number

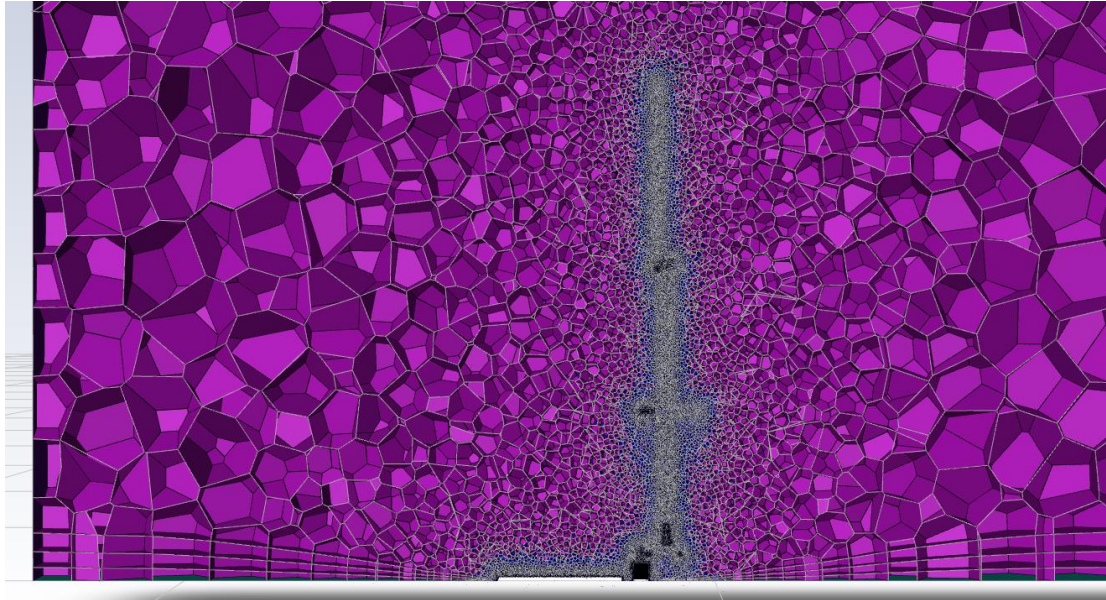


Fig. 9 Analysis Grid setting

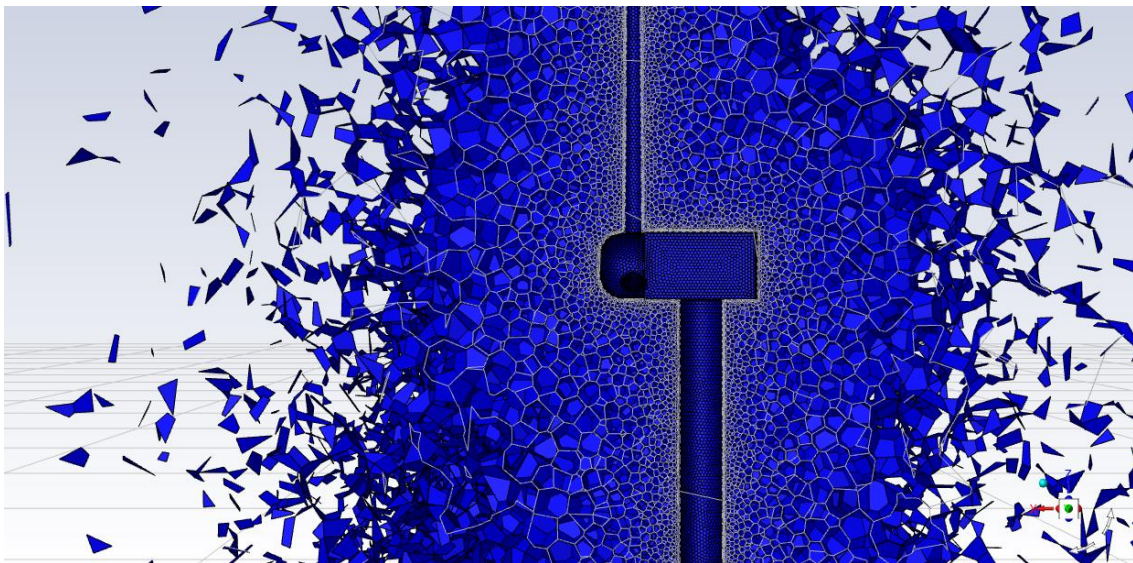


Fig. 10 Analysis Grid setting (close view)

of grids and computational time is shown in Table 6, and an example of the results can be seen in Fig. 11.

The wave force on the vessel analysed in this study does not include linear wave force, as linear wave force has a short-term rapid response that the thrusters cannot adequately address. Additionally, the time-series mean drift force of linear wave force converges to zero. Therefore, linear wave force is not considered.

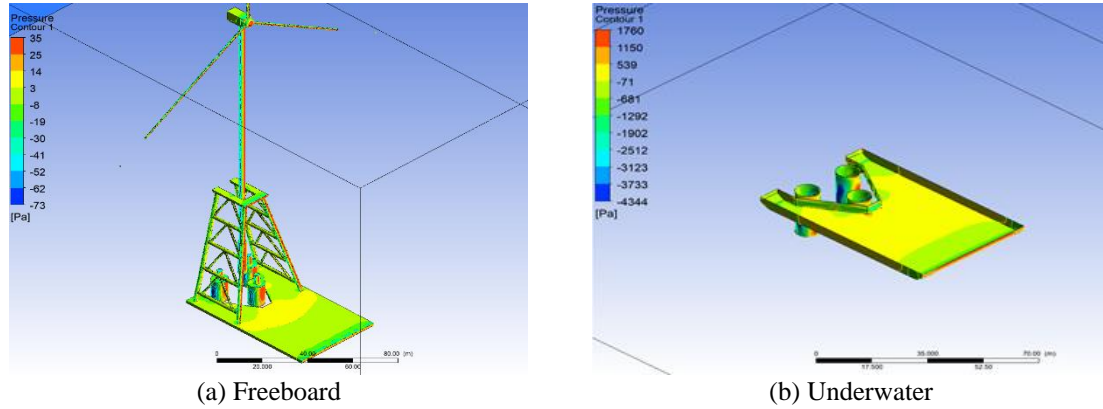


Fig. 11 Pressure distribution

Table 6 Numbers of grids and computational time

Item		Content
Wind model	Average numbers of grids	3189541
	Mean convergence iters	200
	Mean computational time	1600s
Current model	Average numbers of grids	57644
	Mean convergence iters	120
	Mean computational time	480s

For dynamic positioning, the more important wave force is the wave drift force. While wave drift force is smaller in magnitude than linear wave force, its time-series mean drift force does not converge to zero, requiring the vessel positioning system to respond to it. Fortunately, wave drift force has a long-term response, allowing the vessel thrust system to effectively mitigate its effects. Wave drift force can be calculated using the following equations.

Wave drift force can be calculated using the following equations.

$$\overline{F}_i(\psi) = 2 \int_0^\infty S(\omega) H_i(\omega, \psi) d\omega \tag{1}$$

F_i : i -th component of mean drift force in the irregular sea

$S(\omega)$: wave spectrum

$H_i(\omega, \psi) = \overline{F}_i(\omega, \psi) / \zeta_a^2$: i -th component of quadratic transfer function

Typically, the wave spectrum is fixed once the significant wave height ($H_{1/3}$) and modal period (T_0) have been determined. The quadratic transfer function ($H_i(\omega, \psi)$) is also fixed once the shape of the vessel is known. However, in this study, the shape of the vessel is altered during the installation process. Therefore, it was decided to calculate the wave drift force for the vessel in its original shape and then apply the ratio of wave drift force to total resistance for the various altered shapes. To calculate the wave drift force in Analysis state 1. Hull, the wind speed and current speed were taken into account, resulting in a sea state level of 3 and a calculated wave height of 1.3 m. The wave drift

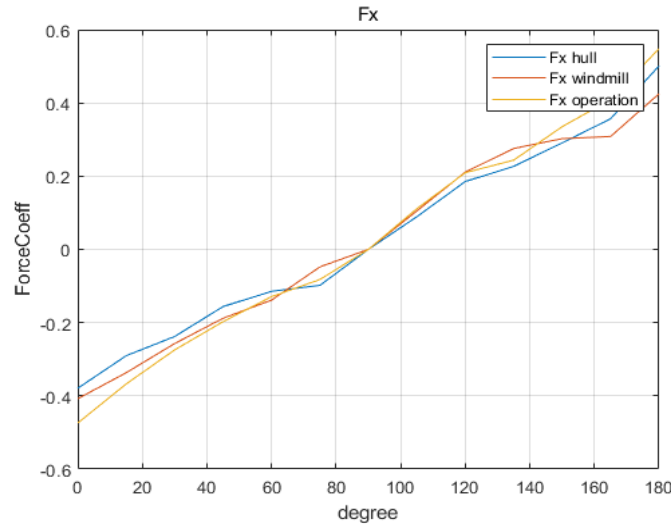


Fig. 12 Current F_x coefficient with angle

force ratio in this case was determined to be 20%. To apply the wave drift force to the other cases, a 20% margin was added to the sum of the wind drift and the current drift.

3.2 Forces acting on the vessel

In this section, the forces acting on the vessel and structures from external forces are shown through changes in the angles and shapes of these forces. These forces can be expressed as follows:

$$F_x = surge, F_y = sway, F_N = yaw \quad (2)$$

Figs. 12-14 depict the coefficients of the forces obtained through analysis of the forces generated when the vessel is influenced by a constant degree of current from 0° to 180° in the surge, sway, and yaw axis, respectively. Figs. 15-17 also show the coefficients obtained through analysis of the forces generated when the vessel receives stable wind power from 0° to 180° in the surge, sway, and yaw axis, respectively. All the power in these figures is expressed as dimensionless coefficients.

$$F_i \text{ coeff} = \frac{F_i}{\frac{1}{2}\rho V_i^2 A_i (LOA)^1} \quad (3)$$

$(LOA)^1$: Length overall uses in yaw Coefficient.

V_i : wind, current speed. uses the speed generated by the relative angle

A_i : the projected area that surge and sway angled plane, fixed for all angle

The coefficient, as defined by the formula, represents the amount of force relative to the area. The vessel being studied is a barge with a square shape both above and below the waterline, resulting in a relatively large coefficient for the hull.

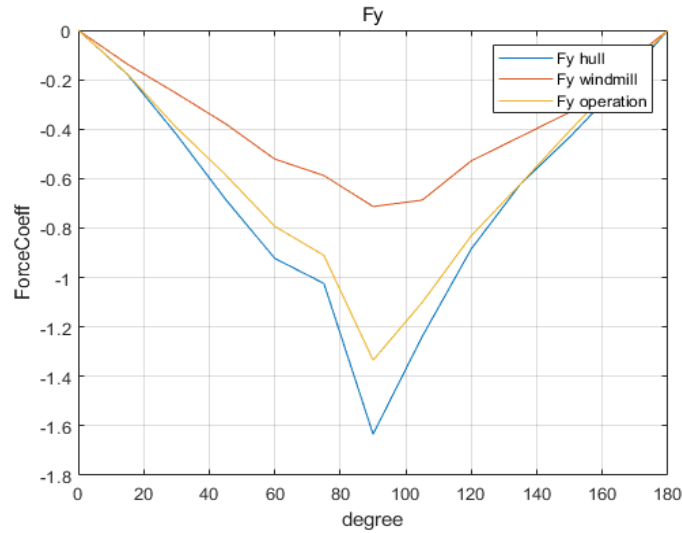


Fig. 13 Current F_y coefficient with angle

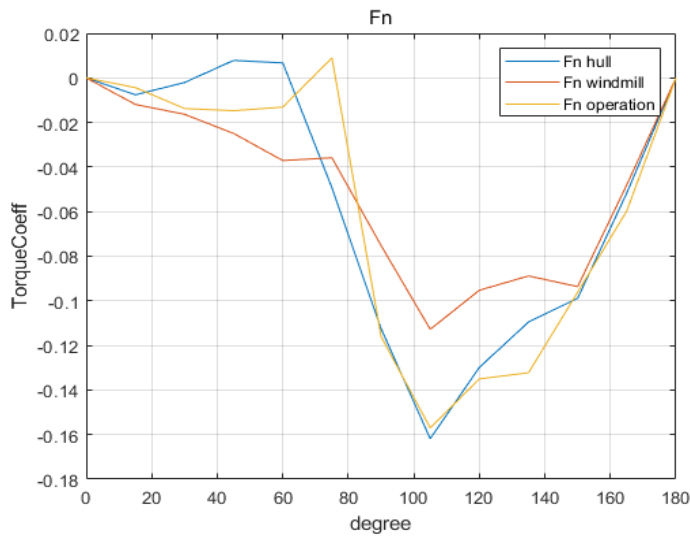


Fig. 14 Current F_N coefficient with angle

The coefficient curve for surge is similar for all angles, indicating that as the size of the projected area increases, resistance also increases linearly. However, in sway and yaw, the coefficients are significantly different due to the discrepancy between the projection area and the actual shape of the wind turbine foundation, which consists of three large cylinders but appears as two cylinders in the projected area.

Additionally, the circular cylinder cuts on the wind turbine towers and support structures result in the hull coefficient in all directions (F_x , F_y , F_N) being larger than those on the wind turbine during loading and operation.

3.3 Dynamic positioning capability plot

For making the capability plot, the dynamic positioning capability of the wind power plant installation was analysed using external environmental force data obtained through CFD. The forces acting on the vessel, as determined in Chapter 4.2, were subtracted from the propulsion force that the vessel could exert in each direction. The experiment was conducted in multiple cases, including three and four propellers, under the conditions of receiving the aforementioned external forces, with power supplies of 1000 kW and 750 kW. The results, shown in Figs. 18-23, demonstrate that maintaining the position of the vessel with only three propellers is challenging, even when the maximum output from the three thrusters is delivered under the same conditions. Therefore, it was concluded that the dynamic positioning system is only effective when four propellers are installed. Additionally, the four-thruster corner case exhibited slightly better position maintenance performance in the 90° and 270° sections, as demonstrated through force correction by moment, compared to the four-thruster case (Valčić 2020).

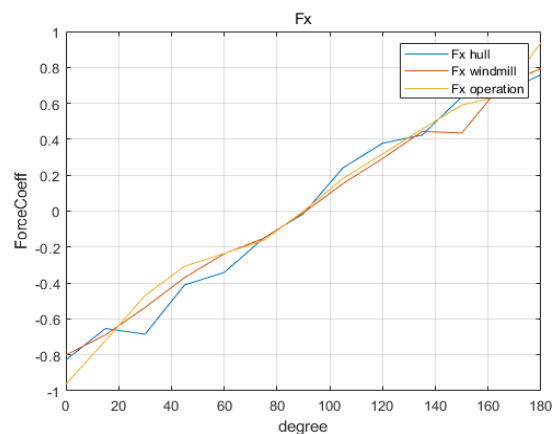


Fig. 15 Wind F_x coefficient with angle

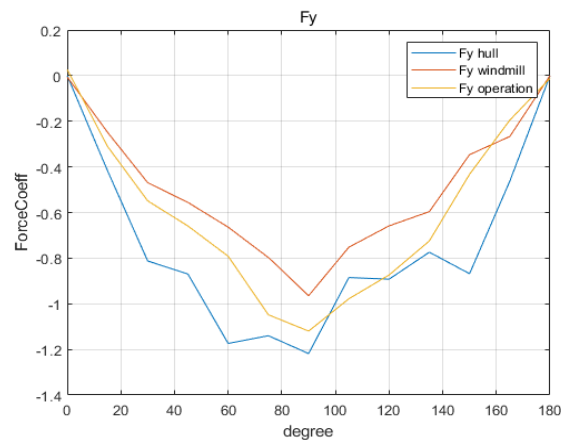


Fig. 16 Wind F_y coefficient with angle

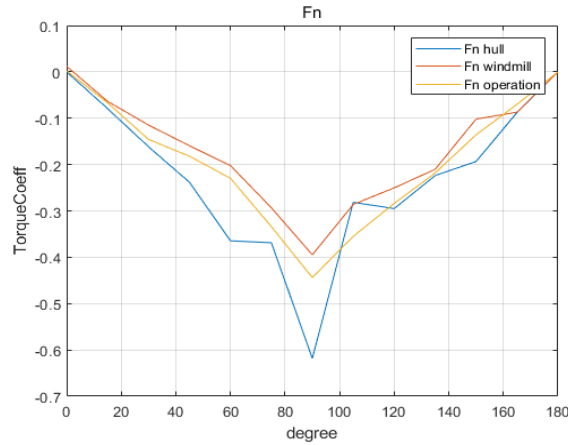


Fig. 17 Wind F_N coefficient with angle

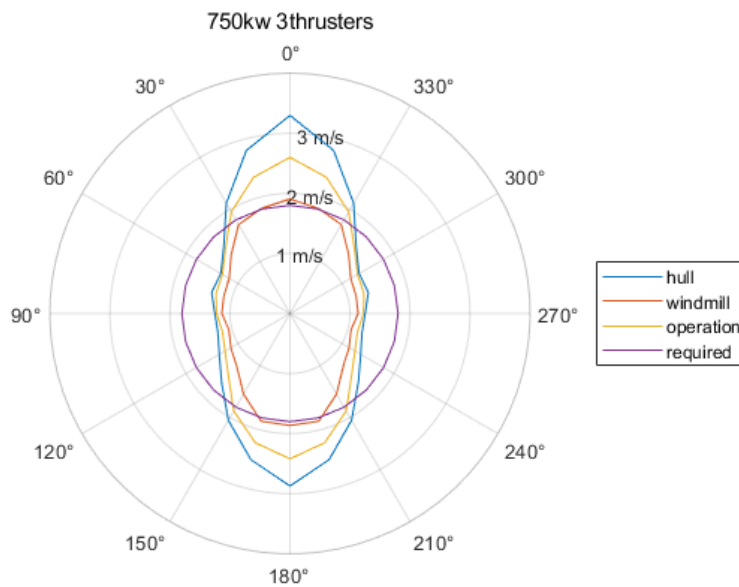


Fig. 18 Capability plot (three thrusters in use of 750 kW)

4. Conclusions

This study analysed the forces exerted on the vessel by external forces acting on the vessel in three different states: an empty load condition, where no load is present on the vessel; an installation condition, where the wind turbine is being installed on the vessel; and an operating condition, in which the vessel with the turbine is afloat and maintaining its position. Using hydrodynamic computation, it was demonstrated that successful DPC during the installation process is not possible unless all four omnidirectional thrusters with a propulsion capacity of 160 kN are installed and

operated. Based on the results of this study, it is proposed that further research should be conducted to estimate more efficient learning algorithms through controller performance analysis of vessels with marine structures, while altering the shapes of the structures at sea. Additionally, the authors are now pursuing research to develop a novel reinforced-learning-based controller that is trained on various shapes that change during operations and exhibits robust control performance.

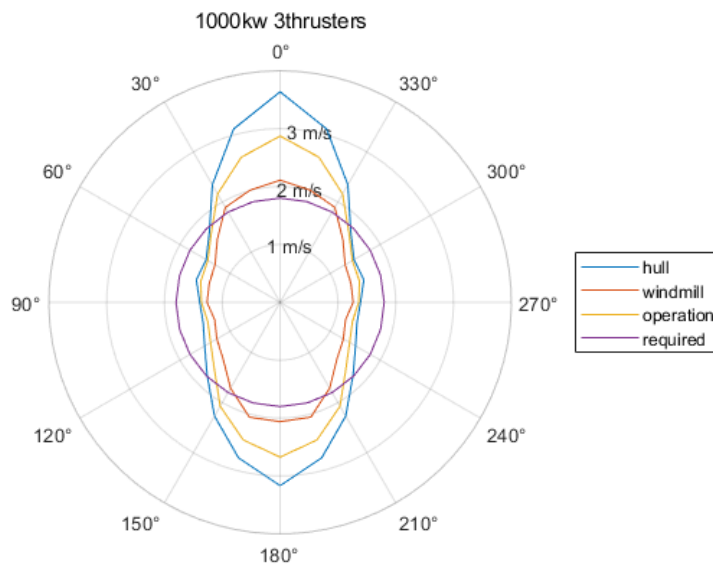


Fig. 19 Capability plot (Three thrusters with a power supply of 1000 kW)

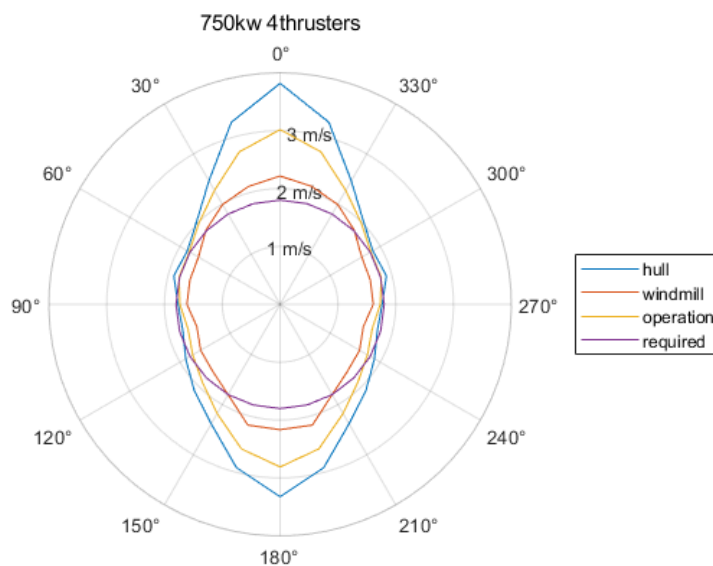


Fig. 20 Capability plot (four thrusters with a power supply of 750 kW)

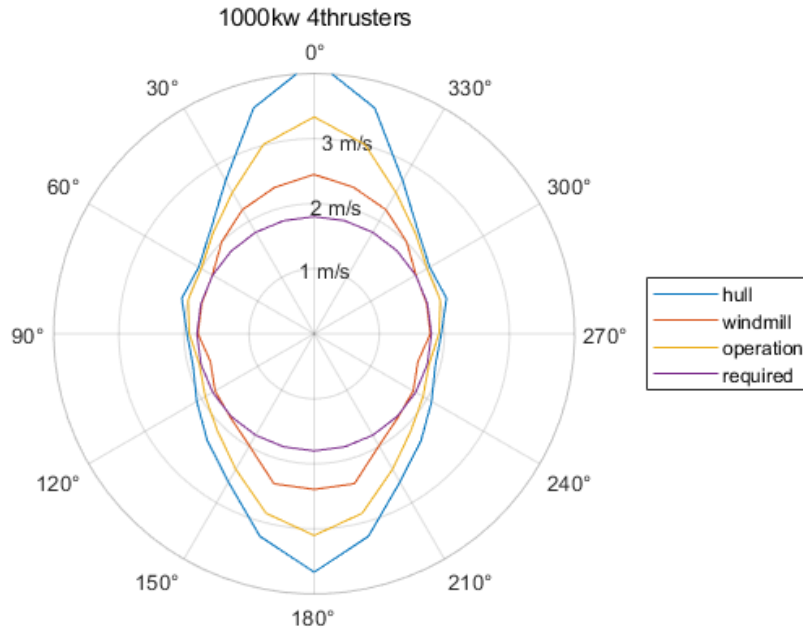


Fig. 21 Capability plot (four thrusters with a power supply of 1000 kW)

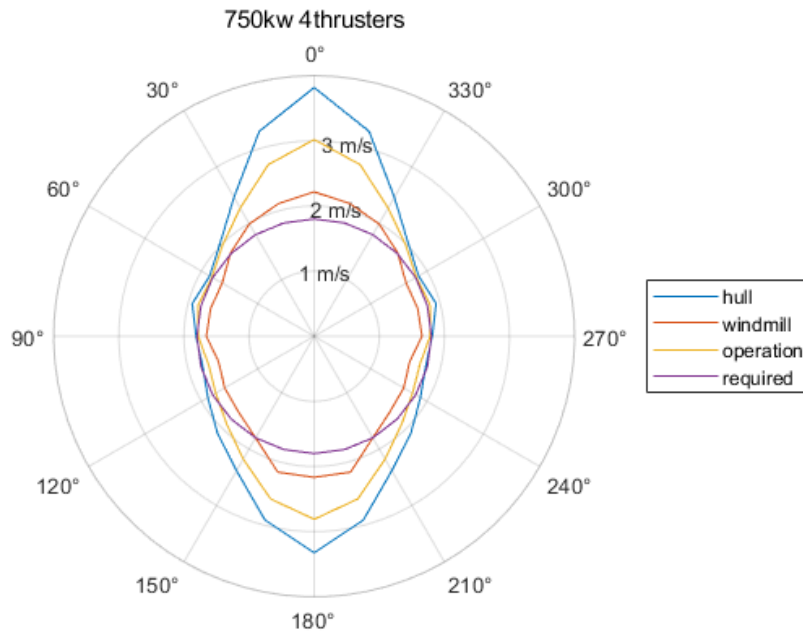


Fig. 22 Capability plot (four thrusters located at the corners of the vessel, with a power supply of 750 kW)

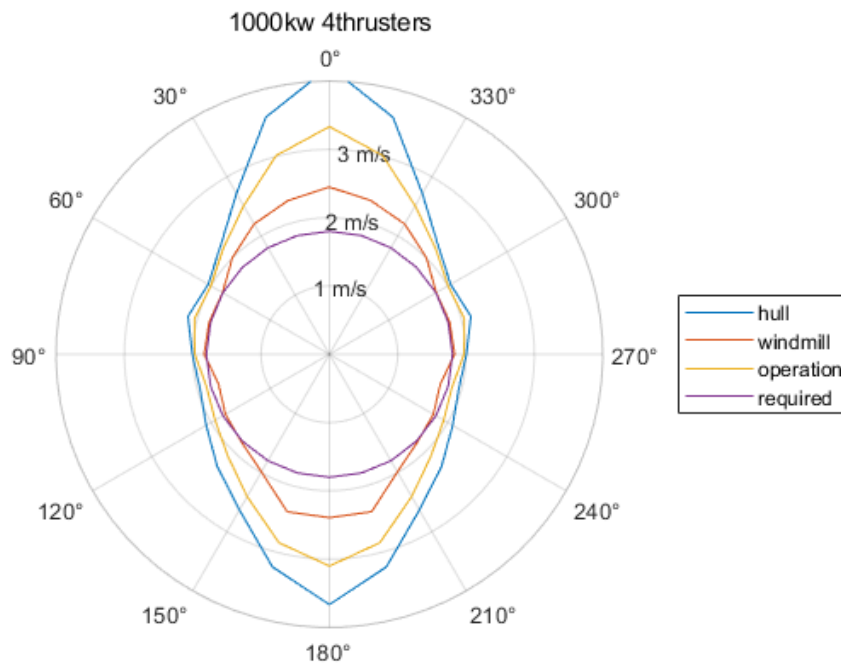


Fig. 23 Capability plot
(four thrusters located at the corners of the vessel, with a power supply of 1000 kW)

Acknowledgments

This research was funded by the MSIT (Ministry of Science and ICT), Korea, under the ICT Challenge and Advanced Network of HRD(RS-2022-00156345) supervised by the IITP (Institute for Information & communications Technology Planning & Evaluation).

References

- Abu Bakar, A. (2019), "Successful float over installation by portable DP vessel", *Proceedings of the Abu Dhabi International Petroleum Exhibition & Conference*.
- Bai, X., Luo, H. and Xie, P. (2020), "Experimental analysis of dynamic response of floatover installation using rapid transfer technique in continuous load transfer process", *J. Mar. Sci. Technol.*, **25**(4), 1182-1198. <https://doi.org/10.1007/s00773-020-00708-7>.
- Choi, J.W., Kim, S.W., Ryu, M.S. and Kim, Y.S. (2012), "Analysis of the effect based on Azimuth Thruster design parameter", *The Korean Society for Marine Environ. Energ.*, 858-863.
- DFI (2017), DFI Announces the 2017 Outstanding Project Award Winners. <https://www.dfi.org/2017/07/05/dfi-announces-the-2017-outstanding-project-award-winners/>.
- Hyakudome, T., Nakamura, M. and Kajiwara, H. (1999), "Experimental study on dynamic positioning control for semi-submersible platform", *Proceedings of the 9th International Offshore and Polar Engineering Conference*.
- Jo, C.H., Kim, S.J. and Cheong, H. (2009), "Dynamic stability during transportation of bridge caisson", *J.*

- Ocean Eng. Technol.*, **23**(1), 104-108.
- Kang, H. and Kim, M. (2014), "Safety assessment of Caisson transport on a floating dock by frequency-and time-domain calculations", *Ocean Syst. Eng.*, **4**(2), 99-115. <https://doi.org/10.12989/ose.2014.4.2.099>.
- Kim, S., Kim, M. and Kang, H. (2016), "Turret location impact on global performance of a thruster-assisted turret-moored FPSO", *Ocean Syst. Eng.*, **6**(3), 265-287. <https://doi.org/10.12989/ose.2016.6.3.265>.
- Kim, S.W. (2016), Eco-Friendly Dynamic Positioning Algorithm Development.
- Mahfouz, A.B. and El-Tahan, H.W. (2006), "On the use of the capability polar plots program for dynamic positioning systems for marine vessels", *Ocean Eng.*, **33**(8-9), 1070-1089. <https://doi.org/10.1016/j.oceaneng.2005.08.006>.
- Mun-Keun, H., (2001), "An experimental method of model installed dynamic positioning system for drillship", *J. Soc. Naval Archit.Korea*, **38**(2), 33-43.
- Paterson, J., D'Amico, F., Thies, P.R., Kurt, R.E. and Harrison, G. (2018), "Offshore wind installation vessels— A comparative assessment for UK offshore rounds 1 and 2", *Ocean Eng.*, **148**, 637-649. <https://doi.org/10.1016/j.oceaneng.2017.08.008>.
- Seok, J., Park, J.C., Heo, J.K. and Kang, H.Y. (2010), "Stability evaluation during transportation of caisson for breakwater", *J. Ocean Eng. Technol.*, **24**(4), 13-22.
- Tahar, A., Halkyard, J., Steen, A. and Finn, L. (2006), "Float over installation method—comprehensive comparison between numerical and model test results", *J. Offshore Mech. Arct. Eng.*, **128**(3), 256-262. <https://doi.org/10.1115/1.2199556>.
- Tannuri, E.A., Agostinho, A.C., Morishita, H.M. and Moratelli Jr., L. (2010), "Dynamic positioning systems: An experimental analysis of sliding mode control", *Control Eng. Practice*, **18**(10), 1121-1132. <https://doi.org/10.1016/j.conengprac.2010.06.007>.
- Tsiropoulos, I., Nijs, W., Tarvydas, D. and Ruiz, P. (2020), "Towards net-zero emissions in the EU energy system by 2050", insights from scenarios in line with the 2030 and 2050 ambitions of the European Green Deal.
- Valčić, M. (2020), Optimization of thruster allocation for dynamically positioned marine vessels, University of Rijeka. Faculty of Engineering.
- Webb, D.L. (1998), "DP and operability capabilities of the dynamically positioned drillship Ocean Clipper", *Proceedings of the IADC/SPE Drilling Conference*.